33RD CONGRESS
OF THE INTERNATIONAL COUNCIL
OF THE AERONAUTICAL SCIENCES
STOCKHOLM, SWEDEN, 4-9 SEPTEMBER, 2022

ICAS 2022 SWEDEN

STEADY-STATE AERODYNAMICS TIP GAP INFLUENCE IN A TRANSONIC LINEAR CASCADE AT NEAR STALL

Carlos Tavera Guerrero [1], Nenad Glodic[1] & Hans Mårtensson[2]

[1]KTH Royal Institute of Technology, Stockholm, Sweden
[2]GKN Aerospace Sweden AB, Trollhättan, Sweden

Abstract

A comparison of steady-state aerodynamics for two tip gap configurations in the KTH transonic linear cascade is presented. The experimental campaign is performed for 1% and 2% tip clearances. The operational point is representative of an open-source virtual compressor (VINK) operating near stall at part speed. The inlet Mach number ($M \approx 0.81$) is above its airfoil critical value with a high incidence angle, producing a leading-edge separation bubble. The measurement plane is at 85% span for each tip gap configuration. Steady-state aerodynamic measurements are presented at the passage and downstream the blades. The blade loading at the passages of interest is mapped by a set of instrumented blades containing 15 pressure taps. The downstream conditions are reconstructed by five-hole probe measurements. Numerical results are computed by the commercial software ANSYS CFX. A comparison of experimental and numerical data is presented to identify correlations and limitations. The scope of this paper is to experimentally and numerically determine the influence of tip gap variation in the steady-state aerodynamics in a transonic linear cascade where leading-edge separation occurs.

Keywords: Steady-state, experimental, linear cascade, CFD, near stall

1. Introduction

In a compressor the tip leakage influences the pressure rise and can be a key driver for an unstable operating point. Bae et al. [1] highlights that the tip leakage generates a blockage in the passage and creates a region of total pressure losses. A correct prediction of tip leakage is critical as it nearly contributes to a third of the compressor stage losses, Denton [2]. Accurate loss predictions by numerical methods is of high relevance, in particular at near stall region. Lejon et al. [3] identified that the losses at the tip region due to a higher blockage led to a adverse impact on such region. The tip clearance flow is highly complex, being inherently unsteady, with pitch-wise and streamwise components, Bae et al. [4]. Tip gap structures are characterized by a leakage roll, creating a concrete vortex structure in the nearby region of blade suction side, and possibly affecting the adjacent blade pressure side. The vortex generation depends on inflow conditions such as turbulence level, boundary layer and vector differences between the main stream and tip leakage jet, as shown by Lakshminarayana [5]. Williams et al. [6] performed large tip clearance variations in a linear cascade, identifying that CFD over-predicts the losses near the casing, and lack of accuracy was observed for small tip gaps. Kang et. al.[7] describes that in a linear compressor cascade, a tip gap increase diminishes the mixing process downstream the tip leakage vortex and this vortex is proportional to the tip gap. Strorer et al [8] states that the blade pressure distribution near the tip is sensitive to the strength and position of the tip leakage vortex, its position is normally at the highest loading and its interaction with the main passage relaxes the corner separation. Nowadays transonic compressor airfoils tend to have a sharp leading edge (LE) at the tip, producing a separation bubble near stall conditions, Liu et al. [9]. Tip leakage and leading-edge induced separation is a common physical phenomena within compressors. Thus this paper aims to investigate the tip gap influence in the steady-state aerodynamics

with 1% and 2% tip gap in a linear cascade at a representative near stall operating point. Numerical results are obtained from the commercial software Ansys CFX, with SST as turbulence model and reattachment method (RM).

2. Test case

At KTH Heat and Power Technology division, a transonic linear cascade (TLC) rig has been designed, shown in Figure 1. The facility aim is to produce reference experimental data for numerical methods validation at a given operational point (OP). The presented OP of interest was recovered numerically and it is representative of a part speed near stall condition of the first rotor of a virtual compressor (VINK) designed by Lejon et al. [10]. The OP had a high inlet Mach number of $\approx$0.81 and an incidence flow angle of $\approx 7^{\circ}$. This paper aims to assess the tip gap influence via numerical and experimental analysis in the steady-state aerodynamics at two tip gaps based on span length, 1% and 2%. Numerical results are obtained from the commercial software Ansys CFX, with SST turbulence model and reattachment method (RM).

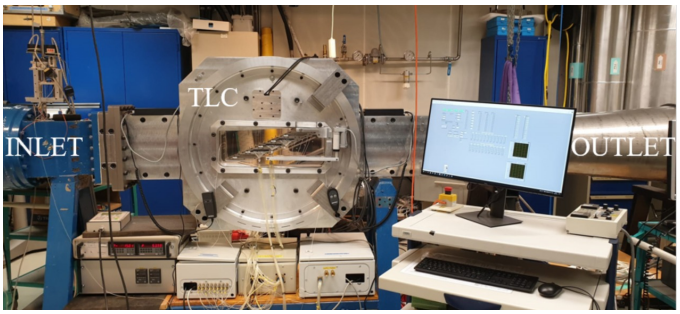

Figure 1 – TLC Assembly.

Fig. 2 shows a cross-section view of the TLC test section, highlighting the blade indexing. The TLC contains five blades staggered at 65°, mounted on a rotating disk for incidence angle modification. Downstream of BP2 and BM2 tailboards are added for periodicity enhancement. The top tailboard is referred as TTB and the bottom tailboard as BTB. A throttle (TH) is mounted on the BTB, to influence BM2 and BM1 passage. Tian et al. [11] performed a CFD aided design of the cascade end-wall contours aiming to produce a periodic flow structures at passages adjacent from B0. The author generated the mechanical design producing slight modifications for manufacturing and instrumentation constraints. The adjacent passage between B0 and BM1 is refer as Passage Minus 1 (PM1), whereas the B0 and BP1 passage is PP1. The experimental setup in which the flow displayed periodic characteristics and representative of the aimed OP for both tip gaps is: 3.5° disk rotation with -1° at BTB, 0° at TTB with 2° TH, refer as experimental reference configuration. At this configuration the relative angle between TTB and BM2 produced a small nominal gap of 0.8mm, refer as TE-bypass.

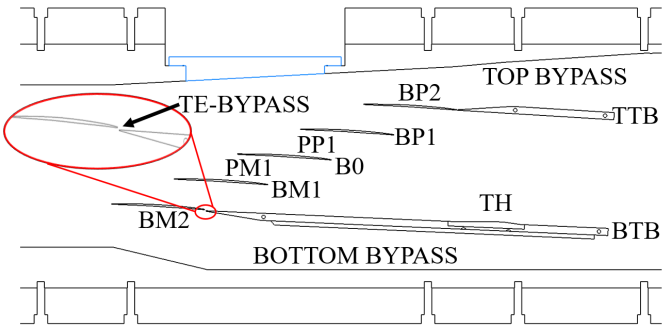

Figure 2 – TLC midspan cross-section with TE-bypass zoom-in.

3. Experimental setup

The blade airfoil corresponds to a prismatic extrusion of VINK first stage rotor airfoil at 95% span. The airfoil has a chord of 104.58 mm and a maximum thickness of 2.04 mm. Steady instrumentation has been performed in the blades at a reference measurement plane (85% span). The instrumented blades have been manufactured with grooves of 0.85 mm by 0.9 mm, in which miniature metal tubes are inserted and aligned with 0.4 mm diameter pressure taps. This process was implemented in 15 locations along the span in regions thicker than 1.1 mm due to manufacture constraints. The grooves are cover with a chemical metal and coating is applied to minimize leakage. Figure 3 presents an instrumented blade and a cross section of the blade at 85% span.

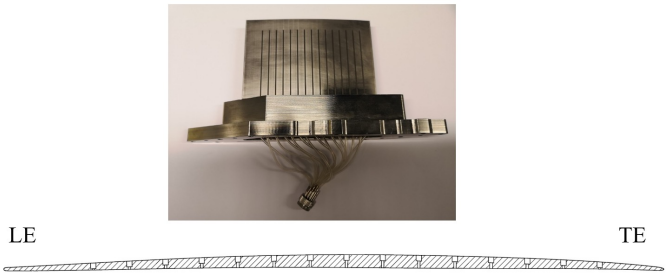

Figure 3 – Instrumented blade at 85% span along blade pressure side.

Tip gap variation was implemented by modifying the hub surface of the prismatic blade. The hub of each blade has been milled to achieve a nominal 1% tip gap (TG). Thus, the blade span for 2% TG is 69.3 mm whereas for 1% TG is 70.0 mm. The experimental tip gap averages are: 1.39 mm $\pm$ 0.05 mm & 0.6 mm $\pm$ 0.05 mm. Tip gap fluctuations are mainly driven due to shroud Plexiglas surface variation. The blade loading of BM1, B0, BP1 were recovered by switching two instrumented blades. After achieving a steady-state condition, the arithmetic pressure was averaged over 5 minutes. All pressures are retrieved by a Pressure Systems PSI, with an uncertainty of $\pm\%$ 0.05 Full Scale [12], at a sampling frequency of 60 Hz with 20 averaged scans. The test section temperature was controlled at 303K $\pm$ 0.5 K. Upstream of the TLC, the total pressure and total temperature ($P_{o_{ref}}$, T_o) are measured at a stagnation chamber.

The OP is mapped by a set of pressure taps distributed in three main regions as shown in Fig. 4. The first, is displayed by green triangle markers, representing the test section inlet. The following, red circles markers represent 11 pressure taps located a quarter chord upstream from the blades along pitch direction. Finally, blue squares show 11 pressure taps located half a chord downstream of blades trailing edge. Each pressure tap along the pitch (75.3mm) is divided into three equal parts. Circles and squares markers are referred in the paper as upstream and downstream locations, respectively.

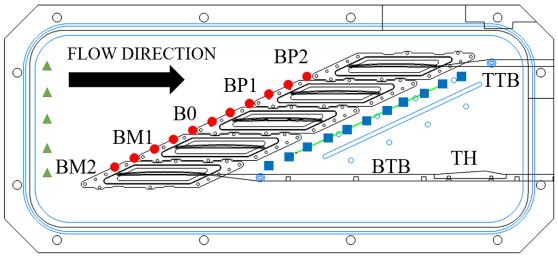

Figure 4 – Pressure taps at the test section inlet (triangles), upstream (circles) and downstream (square).

Downstream, the flow properties are recovered by an in-house designed traverse system for a five-hole probe to measure total pressure, static pressure, Mach number, pitch and yaw angles. The traverse system allows three degrees of freedom: along pitch and span directions, and rotation along the probe axis. The probe has a main stem diameter of 4.9mm with a 43mm L-shape where the measurement stem diameter decreases to 1.6 mm, Fig. 5. The probe is calibrated within KTH facilities in a semi-open configuration. The calibration range is 0.3-0.9 Mach with 0.1 steps, and $\pm\ 20^{\circ}$ for pitch and yaw with 1° steps.

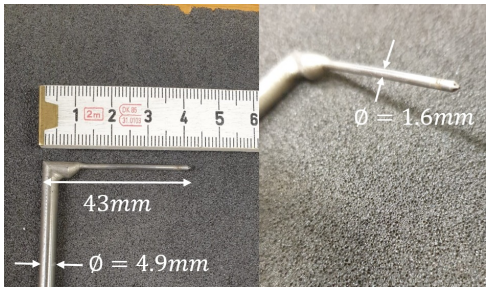

Figure 5 – Five-hole probe stem and head dimensions

A new calibration method was implemented to reconstruct the flow properties. The method showed consistency and reliability to recover the flow properties at high subsonic conditions. The traverse path covers ≈3 normalized pitches centered at B0. Zero represents B0 trailing edge location. A total-total pressure losses coefficient ζ is used as comparison parameter and calculated as Eqn. (1), where $P_{o_{probe}}$ is the reconstructed total pressure and $P_{o_{ref}}$ is the total pressure at the stagnation chamber. A second non-dimensional parameter has been used for comparison, Mach number.

$$\zeta = \frac{P_{o_{ref}} - P_{o_{probe}}}{P_{o_{ref}}} \tag{1}$$

4. Numerical setup

The CFD domain is virtually a 1:1 representation of the TLC assembly, consisting of two contractions, a convergent-divergent nozzle and the test section. All domains are meshed utilizing the commercial software ICEM-CFD due to its robustness and high level of control and mesh quality, Fig. 6.

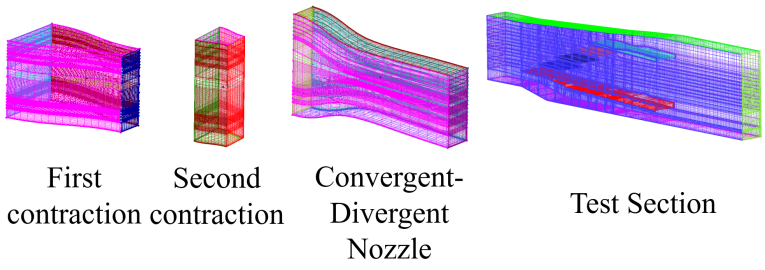

Figure 6 – Discretized experimental domains used in numerical analysis.

The inlet boundary conditions are imposed as a constant value from the measured total pressure in the stagnation chamber of the TLC, and a normal flow velocity is prescribed. The outlet boundary conditions are defined by a blended average static pressure for convergence. The back pressure is controlled numerically by a total-to-static pressure ratio (π) to determine the operational point. The numerical pressure ratio to recover a similar upstream and downstream Mach number is $\pi_{CFD} \approx 1.25$, whereas the experimental $\pi_{Exp} \approx 1.18$, this difference could be associated to multiple sources, e.g.

enforced constant boundary conditions.

The test section domain is of the highest relevance as it contains the blades, tailboards, throttle, and TE-bypass. The test section has been meshed for the experimental configuration in order to have a relevant comparison between numerical and experimental results. Numerically, the tip gap variation has been performed by generating two test sections with different blade heights. The mesh blocking and mesh count are identical except in the span direction, where 1% tip gap needed refinement for convergence. A mesh independence study was performed on each tip gap configuration avoiding mesh influence over the results.

The blade region is meshed by a set of O-grids around the blade to capture the boundary layer separation. The tip gap has been meshed with 21 elements, leading to a $y^+ <\approx 2$ in all blade regions, Fig. 7. The results are obtained by using the commercial software Ansys CFX. The discretized domain consists of $\approx$ 12.8 million elements, where the test section contains $\approx 95\%$ of the total amount of elements. The test section has two high refinement regions, the first is nearby the LE of each blade to capture the separation bubble. The second, is along the blade tip in spanwise direction to capture the tip gap effect over the plane of interest. The selected turbulence model is SST with turbulence reattachment modification (RM). This method has been chosen as currently a turbulent transition ($\gamma - \theta$) cannot be applied in moving meshes and RM has a stronger agreement with experimental data than a standard SST.

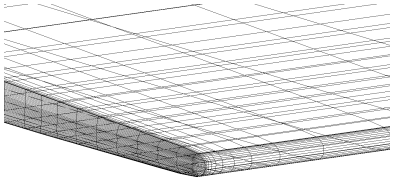

Figure 7 – Meshed blade tip zoom-in.

5. Results

5.1 Blade loading

Fig. 8 displays the upstream and downstream isentropic Mach number (M_s) against the normalized pitch upstream for both tip gaps. Integer values along the x-axis represent the pitch location of BM1, B0 and BP1. The shown data corresponds to an average over three independent experiments at the same operational point. A key difference between figures 8a and 8b is the increased Mach number trend towards 1.5 normalized pitch. An increase of blade height (1% TG) produced a higher blockage over the cross-section of the TLC, thus a higher mass flow is required to achieve the same operational point as for 2% tip gap configuration.

In both figures there are drops of Mach number at positions upstream BM1, B0 and BP1. These drops are due to the potential effect of a weak normal shock along the SS of the adjacent blade. For instance at 0 normalized pitch (B0), the drop of Mach corresponds to BM1 normal shock. This normal shock is the main mechanism for a strong adverse pressure gradient to induce a separation bubble. Similarly, sub figure 8b shows slightly stronger shocks on the previously described region, possibly affecting the flow structure upstream the blades. The passage between BM2 and BM1 shows a stronger Mach gradient from 0.73 to 0.85 rise and it is slightly affected by the tip gap. It is assumed that this region is mainly dominated by the potential effect of the bottom bypass and thus less sensitive to the tip gap.

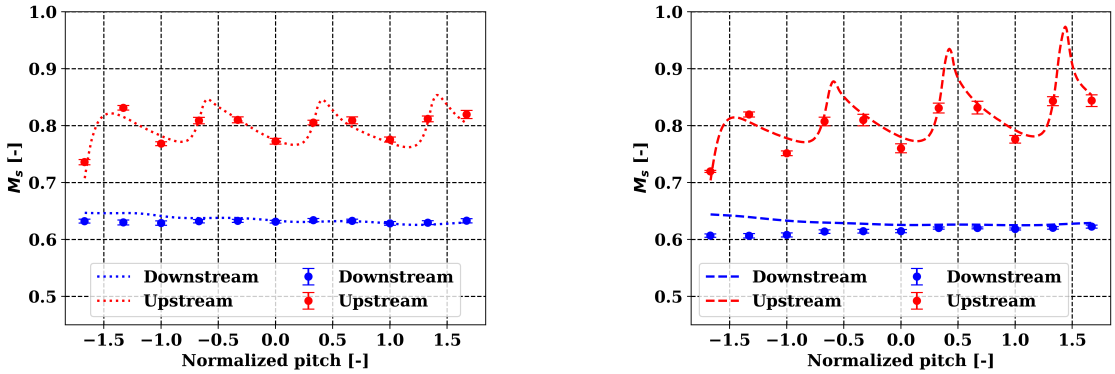

(a) Operating point at 2% TG

(b) Operating point at 1% TG

Figure 8 – Experimental and numerical upstream-downstream isentropic Mach number at different tip gaps.

A second qualitative difference is that at 2% tip gap the trend of upstream condition shows a relatively even distributed pattern along the pitch, inferring better upstream periodicity than a 1% tip gap. Downstream conditions for both cases show a similar mean value, whereas the a slight different trend is observed for 1% tip gap. A small increase in Mach number towards positive blade indexes is appreciated experimentally. It is assumed that this effect is driven by the upstream increase of inlet Mach number, however this is not predicted by the numerical analysis. It is apparent that both operating points have a similar downstream conditions along the measured region.

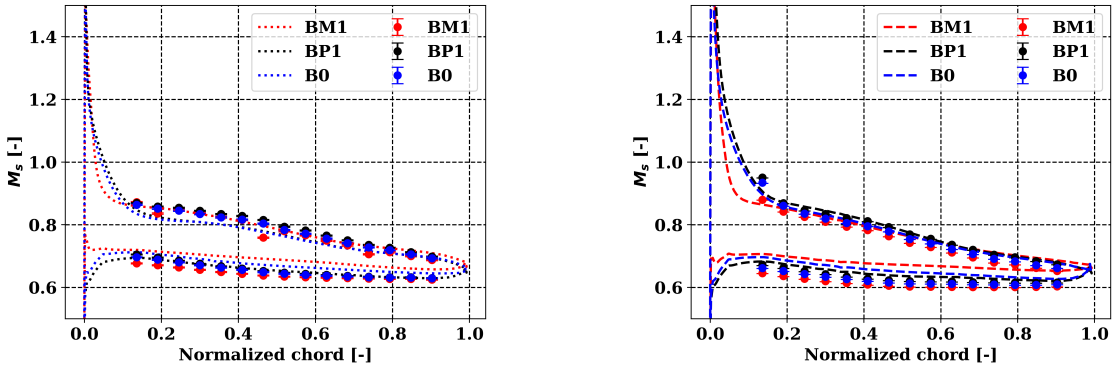

(a) M_s vs normalized chord at 2% TG

(b) M_s vs normalized chord at 1% TG

Figure 9 – Experimental and numerical M_s comparison: 2% TG (Left), 1% TG (Right).

Figure 9 shows the experimental and numerical blade loading of blades BM1, B0 and BP1 against its normalized real chord. The dashed and dotted lines represent CFD results and discrete points represent the experimental data with the error bar corresponding to two standard deviations. The experimental results in subfigure 9a shows a relatively good agreement in terms of periodicity for all the three blades. Slight differences occur in the PS and in the aft region along the SS, suggesting that the flow field at each blade is similar but it is possible that the flow structures at each passage might differ significantly as the pressure at the wall is constant throughout the boundary layer and depending only on the inviscid region. For this case, CFD predicted blade loading provides a qualitative agreement in particular at the SS but slighter differences are found at the PS. Numerical results display noticeable differences in the first 20% of the chord SS and along the chord PS. This observations suggest that the flow field predicted numerically has lower degree of periodicity compared to the experiments.

On the other hand subfigure 9b shows a higher loading with a stronger adverse pressure gradients in the first two taps of the blade SS, where BP1 and B0 have an apparent higher incidence angle. Due to a higher inlet Mach number there might be a stronger bottom bypass blockage effect. However

this effect would be stronger on BM2 and BM1, but B0 and BP1 appear to have a similar flow, most likely driven by the tip gap effect.

Numerical results predict a qualitative agreement with experimental data, in particular for 2% TG, where the flow conditions in the adjacent passages to B0 is similar. It is observed that for the smallest tip gap at the same regions the Mach number from passage to passage varies. This observation is predicted by CFD, suggesting that the shocks in the passage are becoming stronger as moving towards BP1, producing a lower degree of periodicity. Finally, CFD does not predict a constant pressure region, characteristic of separated flow, nevertheless the velocity field displays separation in the fore region of the SS (results not shown).

From this comparison it is hypothesized the experimental measurements resembles a higher degree of periodicity than predicted numerically, as the blade loading appears to have a periodic behavior within the limitations of a linear cascade. In order to confirm or falsify the hypothesis, a different method is required due to pressure tap instrumentation constraints. Additionally, it is observed that CFD indicates higher differences in both PS and SS for all configurations, inferring a certain degree of discrepancy between CFD and experiments.

5.2 Five-hole probe results

This section highlights the results from a five-hole probe measurements at half a chord downstream from the blades for both tip gap configurations. Both cases were post-processed by the same procedure and the experimental data was recovered by the same method. The probe moved to approximately 3 pitches centered at B0 and covering an area from 85% span to 90% for 2% TG and from 50% to 90% from 1% TG. For a 2% TG configuration the probe motion showed clear effects on the flow field when traversed lower than 85% span, whereas for 1% the probe effect was negligible up to 50% span. Figure 10, displays the reconstructed Mach number and Total pressure loss (ζ) for both cases from 85% to 90% span.

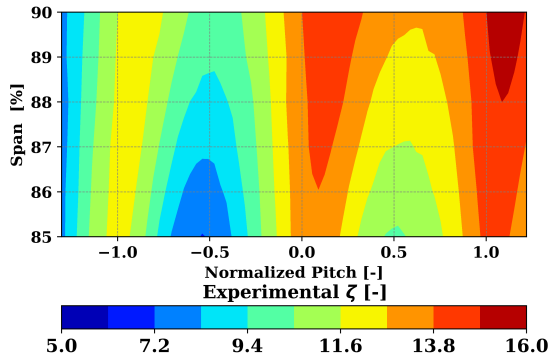

(a) Experimental ζ: 2% TG

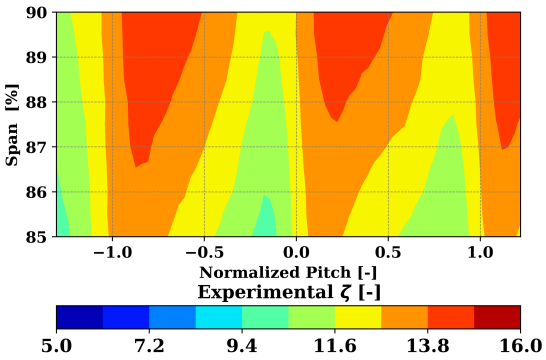

(b) Experimental ζ: 1% TG

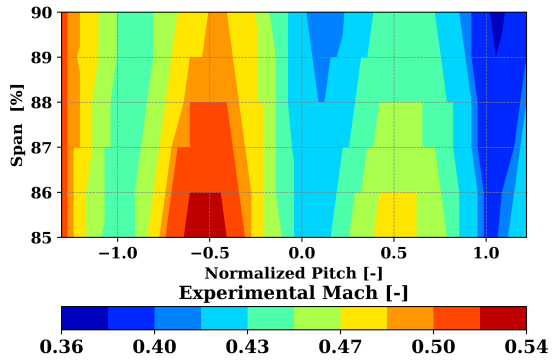

(c) Experimental Mach number: 2% TG

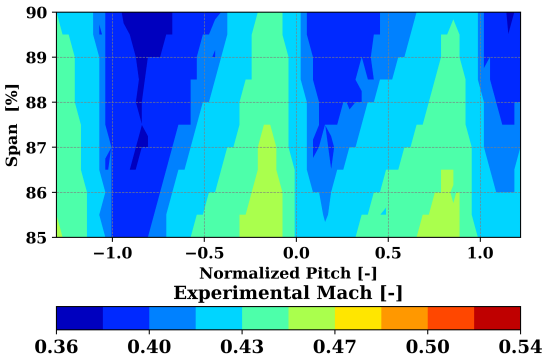

(d) Experimental Mach number: 1% TG

Figure 10 – Experimental total pressure loss and Mach number at different tip gaps

Subfigures 10a & 10b display the experimental total pressure loss for both cases with a clear qualitative difference between tip gaps. At 2% TG the maximum and minimum losses are occurring. The highest nearby the tip region and the smallest is observed in the passage between BM1 and B0. In subfigure 10a it is assumed that in regions lower than -1 normalized pitch the TE-bypass is adding momentum along the span and thus no increase of loss is clear towards the tip, the low loss region might be due to the TE-bypass interacting with the main stream. Regions higher than this position are due to the tip gap vortex being transported and dissipated downstream. It is observed that for 1% TG there are clearer structures with higher losses towards the tip of the adjacent blade with negative indexing. This behavior indicated a curling of the tip leakage vortexes that are being transported downstream. This mechanism is consistent for each blade and the highest region of losses correspond in the nearby region of BM1 SS. Similarly, towards the tip losses increase and it is believed that the TE-bypass is having virtually no effect over the measured region.

Subfigures 10c & 10d display a similar qualitative trend as the total pressure loss, where there is an overall lower Mach number at 1%TG due to the tip leakage vortex. This trend is not captured for 2% TG configuration, where a region up to 0.54 in Mach number is predicted for the passage between BM1 and B0. It is apparent that a change in tip gap lead to a different flow field structures in the mapped region, in particular nearby the TE-bypass, where the flow structures for 1% TG appear to have a stronger apparent periodicity compared to 2% TG. This preliminary conclusion is counter intuitive from figures 8 & 9 where 2% TG displays a stronger periodic behavior upstream and at the blade loading. This observation suggests that a tip gap reduction enhances the periodic characteristics downstream the blades suggesting that the flow in the adjacent passages has similar structures.

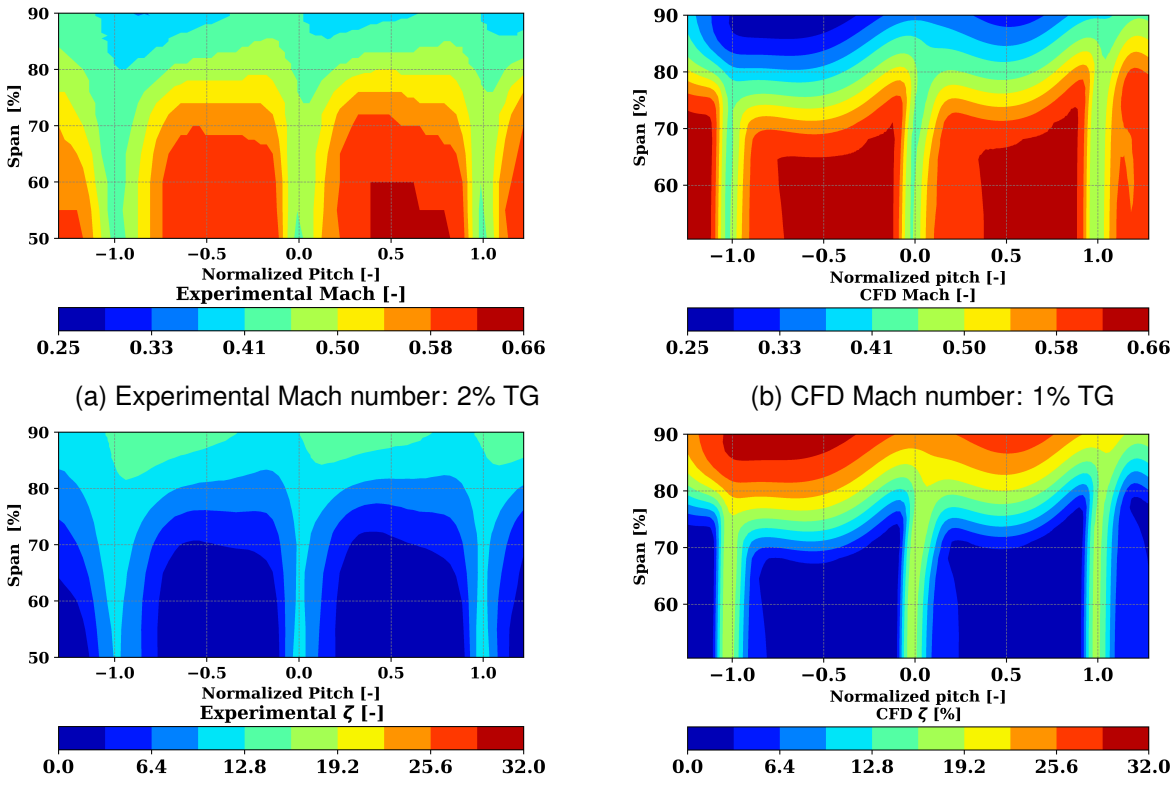

(a) Experimental Mach number: 2% TG

(b) CFD Mach number: 1% TG

(c) Experimental ζ: 1% TG

(d) CFD ζ: 1% TG

Figure 11 – Mach number and ζ numerical and experimental comparison at 1% tip gap

Figure 11 exhibits the pressure loss and Mach number from 50% span to 90% for 1% TG configuration. Subfigures 11a & 11b display the Mach number half a chord downstream. CFD over-predicts a low momentum region nearby the tip of -1 normalized pitch, corresponding to the tip leakage from B0. The low momentum region is significantly different from Mach 0.25 numerically to Mach 0.32

experimentally. Both methods predict that the tip leakage vortex is affecting above 70% span at the adjacent passages from B0. Below 70% span, the downstream conditions show periodic characteristics an the recovered Mach number is in agreement with the downstream values from figure 8, providing a higher degree of confidence in the reconstruction data methodology.

Subfigures 11c & 11d display the experimental and numerical pressure loss. Despite both methods predicting a similar strength of the tip gap along the span, the tip leakage vortex from SS to PS shows a different trend than the observed experimentally. Furthermore, CFD tip leakage losses are double than the experimental, displaying that the current turbulence model is over-conservative. This behavior is not found at the wakes, where the loss difference is from 12.8% to 16% by CFD, showing the complexity of an accurate prediction of tip leakage.

6. Conclusions

An experimental and numerical comparison due to tip gap influence inside a transonic linear cascade representative of a near-stall operating point has been presented. The main findings are as follows:

- A tip gap decrease produced a larger blockage in the cross-section of the TLC and more mass flow was required to achieved a similar operating point for both configurations leading to a lower degree of periodicity at upstream Mach number for 1% TG. Numerical predictions at upstream conditions are in agreement with the experimental data.
- Experimental blade loading shows a higher degree of periodicity for BM1, B0 and BP1, than CFD predictions for both tip clearances. The smaller tip clearance appears to modify the incidence angle producing a higher adverse pressure gradient.
- The numerical isentropic Mach number predicts a normal shock in the first 10% of the chord but no clear sign of a typical separated region is observed. The separation mechanism is apparently dominated by the adverse pressure gradient due to the shock.
- Downstream five-hole probe results show that 2% TG configuration has a significantly lower degree of periodicity at the passages adjacent to B0. The passage between BM1 and B0, contains a high momentum region possibly driven by the TE-bypass. At 1% TG shows a higher degree of periodicity, where the higher losses are concentrated in regions where the tip gap vortex is being transported. The pressure losses are higher at the largest tip gap in regions towards the tip.
- For 1% tip gap both experimental and numerical results predict that the tip leakage vortex influences $\approx 30\%$ of the blade tip. The tip leakage losses predicted by CFD displays a qualitative agreement but there is a quantitative mismatch as numerical total pressure loss is two times higher than the observed experimental data.
- Further experimental data is required to identify a separation region such flow visualization via oil-based paint over the blades of interest. Flow field mapping inside the passages of interest is advice for a better understanding of the sources of losses, and its effect at the measurement plane.

7. Contact Author Email Address

Contact details, mailto: catg@kth.se, nenad.glodic@energy.kth.se, hans.martensson@gknaerospace.com

8. Copyright Statement

References

[1] Jin Woo Bae, Kenneth S. Breuer, and Choon S. Tan. Active Control of Tip Clearance Flow in Axial Compressors . *Journal of Turbomachinery*, 127(2):352–362, 05 2005.

[2] J Do Denton. *Loss mechanisms in turbomachines*, volume 78897. American Society of Mechanical Engineers, 1993.

[3] Marcus Lejon, Tomas Grönstedt, Niklas Andersson, Lars Ellbrant, and Hans Mårtensson. On improving the surge margin of a tip-critical axial compressor rotor. Volume 2A: Turbomachinery, 06 2017.

[4] Jinwoo Bae, Kenneth S Breuer, and Choon S Tan. Periodic unsteadiness of compressor tip clearance vortex. In *Turbo Expo: Power for Land, Sea, and Air*, volume 41715, pages 457–465, 2004.

[5] B. Lakshminarayana, M. Zaccaria, and B. Marathe. The Structure of Tip Clearance Flow in Axial Flow Compressors. *Journal of Turbomachinery*, 117(3):336–347, 07 1995.

[6] Richard Williams, David Gregory-Smith, Li He, and Grant Ingram. Experiments and Computations on Large Tip Clearance Effects in a Linear Cascade. *Journal of Turbomachinery*, 132(2), 01 2010.

[7] S. Kang and C. Hirsch. Tip Leakage Flow in Linear Compressor Cascade. *Journal of Turbomachinery*, 116(4):657–664, 10 1994.

[8] J. A. Storer and N. A. Cumpsty. Tip Leakage Flow in Axial Compressors. *Journal of Turbomachinery*, 113(2):252–259, 04 1991.

[9] Huo-xing Liu, Bao-jie Liu, Ling Li, and Hao-Kang Jiang. Separation bubble around a leading edge of compressor blade. In *Optical Technology and Image Processing for Fluids and Solids Diagnostics 2002*, volume 5058, pages 199–207. International Society for Optics and Photonics, 2003.

[10] Marcus Lejon, Tomas Grönstedt, Nenad Glodic, Paul Petrie-Repar, Magnus Genrup, and Alexander Mann. Multidisciplinary design of a three stage high speed booster. In *Turbo Expo: Power for Land, Sea, and Air*, volume 50794, page V02BT41A037. American Society of Mechanical Engineers, 2017.

[11] Simeng Tian, Paul Petrie-Repar, Nenad Glodic, and Tianrui Sun. Cfd-aided design of a transonic aeroelastic compressor rig. *Journal of Turbomachinery*, 141(10), 2019.

[12] Jens Fridh. Calibration trials of rapid prototyping probes. Technical report, KTH, EKV 05/10, 2010.